RESEARCH ARTICLE

Dielectric Properties of Lead-Free (1-x)$SrTiO_3$-x$CaZrO_3$ Solid-Solution Ceramics Prepared by Solid-State Sintering

Basit Ahmad[1] **and Akbar Khan**[1,*]

[1] Department of Physics, Abdul Wali Khan University Mardan, Mardan 23200, Pakistan

Abstract

Lead-free (1-x)$SrTiO_3$-$x$$CaZrO_3$ solid-solution ceramics (x = 0.05, 0.10, 0.15, 0.20) were synthesized via the conventional solid-state route to investigate structure-microstructure-dielectric relationships. X-ray diffraction patterns of the samples confirmed single-phase formation for all compositions, forming cubic perovskite structure (space group $Pm-3m$). Raman spectra were consistent with the perovskite lattice and local vibrational features, confirming perovskite structure. SEM micrographs revealed noticeable porosity for lower $CaZrO_3$ contents (x = 0.05-0.15) and a more compact morphology at higher $CaZrO_3$ content, with a slight decrease in grain size as x increases (average grain size $\approx$ 0.49 μm). Dielectric measurements show pronounced frequency dispersion: the relative permittivity decreases with increasing frequency, consistent with dielectric relaxation behavior. Increasing $CaZrO_3$ content decreases the relative permittivity and decreases dielectric loss. The $x = 0.20$ sample showed reduced low-frequency loss, consistent with improved resistivity and densification. These results show that composition control in the $SrTiO_3$-$CaZrO_3$ system provides a practical route to tailor dielectric response in lead-free perovskite ceramics.

Keywords: $SrTiO_3$-$CaZrO_3$, solid solution, perovskite ceramics, dielectric constant, dielectric loss, dielectric relaxation, solid-state sintering, lead-free dielectrics.

1 Introduction

Perovskite oxides with the general formula ABO_3 are widely studied as dielectric ceramics because their crystal framework is chemically stable and can accommodate extensive compositional tuning [1, 2]. This flexibility enables the optimization of dielectric constant, dielectric loss, and electrical resistivity required for multilayer ceramic capacitors, sensors, actuators, and microwave components. Among the perovskite structures, $SrTiO_3$ (STO) has been widely investigated for microwave and high-voltage dielectric applications because it can combine a relatively high permittivity with low loss when processed appropriately [3–5]. Its dielectric response is strongly influenced by defect chemistry and processing history. In particular, oxygen vacancies

Submitted: 21 February 2026
Accepted: 27 March 2026
Published: 02 April 2026

Vol. 2, **No.** 2, 2026.
10.62762/JAEM.2026.626525

***Corresponding author:**
✉ Akbar Khan
akbar.khan@awkum.edu.pk

Citation
Ahmad, B., & Khan, A. (2026). Dielectric Properties of Lead-Free (1-x)$SrTiO_3$-x$CaZrO_3$ Solid-Solution Ceramics Prepared by Solid-State Sintering. *Journal of Advanced Electronic Materials*, 2(2), 38–43.

© 2026 by the Authors. Published by Institute of Central Computation and Knowledge. This is an open access article under the CC BY license (https://creativecommons.org/licenses/by/4.0/).

can produce low-frequency dielectric relaxation and can contribute to electrical conduction and loss, while aliovalent doping can further tune these behaviors [6, 7]. Such defect-related relaxation has been reported in modified STO-based ceramics, where the relaxation and conductivity trends are often linked to oxygen-vacancy migration and related transport processes [8, 9]. Because leakage and dielectric loss typically increase under conditions that promote defect conduction, controlling defects and microstructure is central when STO-based ceramics are considered for energy-storage dielectrics. Similarly, $CaZrO_3$ (CZO) is another perovskite oxide of interest for dielectric applications due to its high thermal and chemical stability and its potential for low-loss dielectric performance [10]. Structural studies describe CZO as a perovskite system with temperature-dependent polymorphism and perovskite-type octahedral frameworks that can host defects and dopants relevant to electrical transport [11, 12]. CZO ceramics have also been investigated as dielectric materials for multilayer capacitor concepts and microwave dielectrics, supporting its use as a functional component in perovskite dielectric design [13, 14]. Within this context, combining STO and CZO through a solid-solution or composite approach provides a route to tune lattice chemistry, defect sites, and microstructure together. Recent work on CZO-STO-based ceramics reports high-temperature dielectric relaxation and energy-storage-relevant dielectric behavior, indicating that composition can be used to modify dielectric response and loss characteristics [15]. Therefore, in this study, lead-free $(1\text{-}x)$STO-xCZO ceramics with $x = 0.05$, 0.10, 0.15, and 0.20 were fabricated by a conventional solid-state route and examined to establish composition-structure-microstructure-dielectric relationships relevant to dielectric and energy-storage applications.

2 Experimental procedure

Lead-free $(1\text{-}x)$STO-xCZO ceramics with $x = 0.05$, 0.10, 0.15, and 0.20 were synthesized using a conventional solid-state route. Reagent-grade $SrCO_3$, TiO_2, $CaCO_3$, and ZrO_2 powders ($> 99.0\%$, Sigma Aldrich) were dried at 200 °C to remove absorbed moisture and then weighed according to the required stoichiometry. The weighed batches were mixed and milled in acetone for 1 h using an agate mortar and pestle to limit contamination. The mixed powders were calcined at 1000 °C for 6 h in an alumina crucible to complete the reaction and remove carbonate species, followed by re-milling to break agglomerates. The calcined powders were uniaxially pressed into pellets using an 8 mm die (typical pellet thickness ≈ 1 mm and diameter ≈ 7 mm) at a nominal pressure of 100 MPa and then sintered in an alumina (corundum) crucible using a muffle furnace. The sintering schedule is reported as 1375–1400 °C for 8 h, with the principal set sintered at 1400 °C for 8 h to densify the ceramics through diffusion-driven mass transport during electro-ceramic sintering.

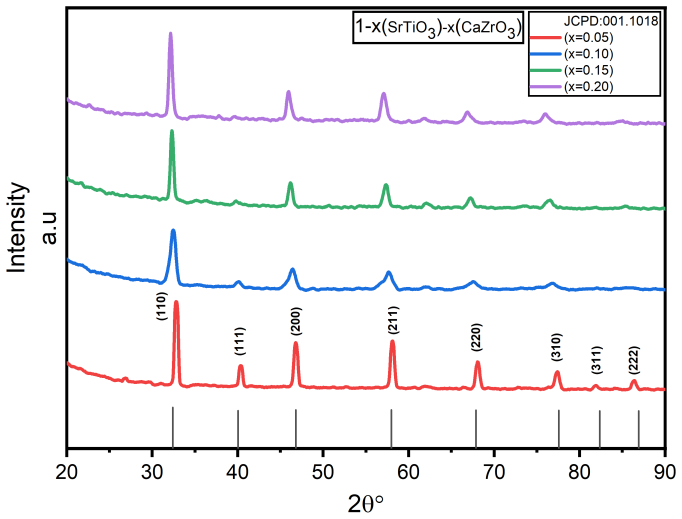

Figure 1. X-ray diffraction patterns of $(1\text{-}x)$STO–xCZO with $x = 0.05$, 0.10, 0.15, and 0.20 ceramics.

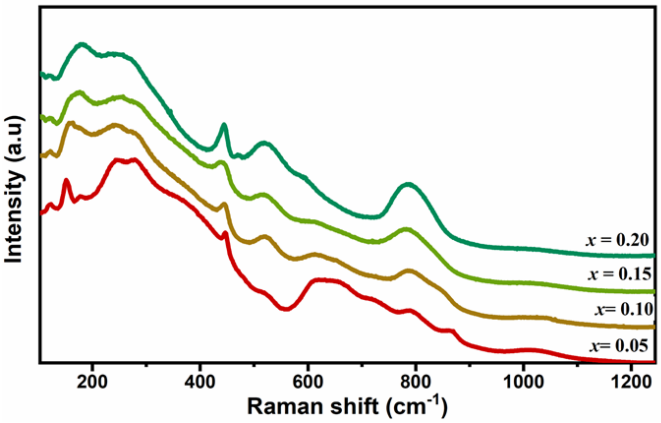

Figure 2. Raman spectra of $(1\text{-}x)$STO–xCZO with $x = 0.05$, 0.10, 0.15, and 0.20 ceramics samples.

Phase formation and crystal structure were examined by powder X-ray diffraction using Cu Kα radiation over $2\theta = 20°$–$80°$ on an AXRD LPD Proto Powder X-ray diffractometer (GIKI, Pakistan), and d-spacings were evaluated using Bragg's law. Raman spectra were recorded at room temperature using a MultiRAM FT-Raman spectrometer (Bruker, Germany) with 1064 nm Nd:YAG excitation and a spectral resolution of 4 cm^{-1}. Microstructures were examined on polished

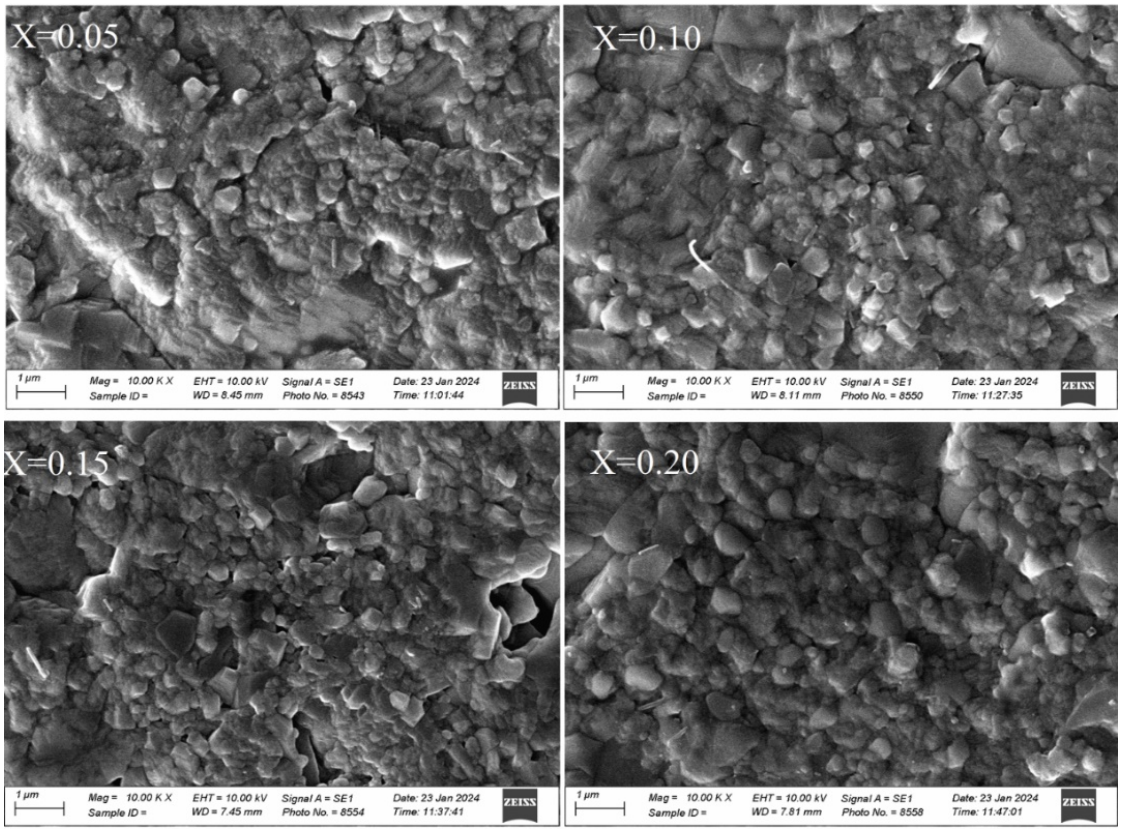

Figure 3. SEM images of the $(1\text{-}x)$STO–xCZO $(x = 0.05\ 0.20)$ ceramic samples sintered at 140°C.

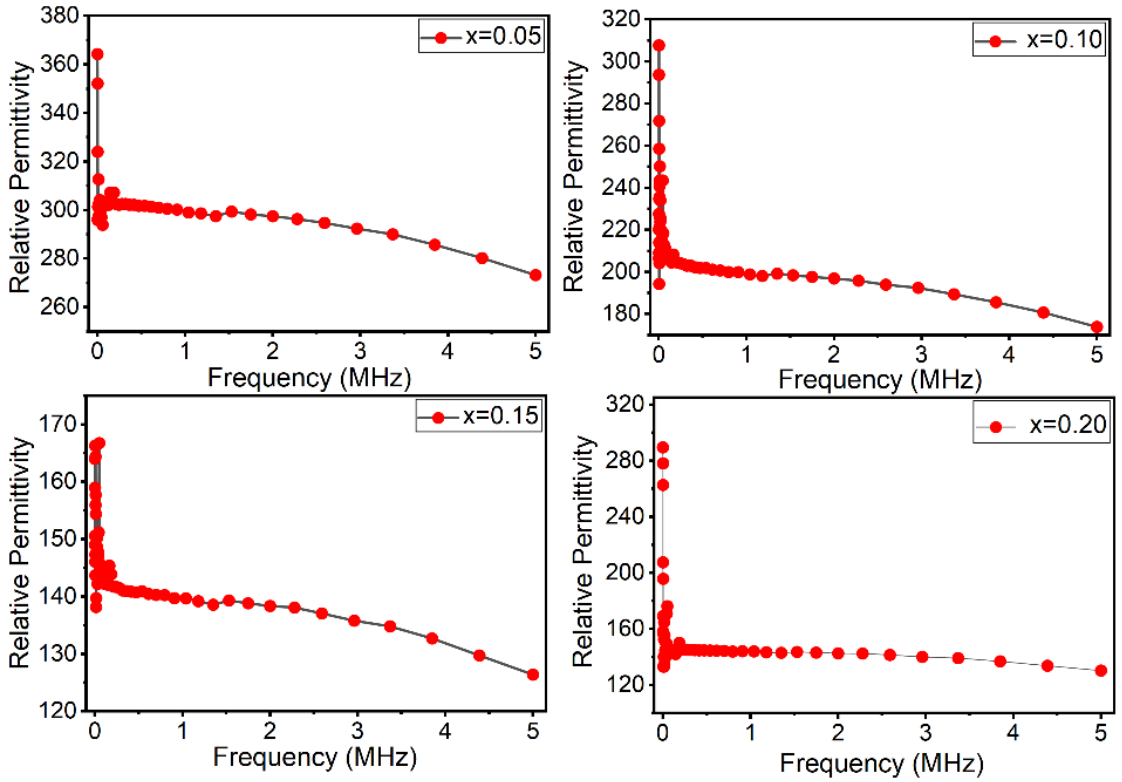

Figure 4. Relative permittivity of ceramic sample $(1\text{-}x)$STO–xCZO $(x = 0.05, 0.10, 0.15, 0.20)$.

and thermally etched surfaces using SEM (Carl Zeiss EVO 15, W-filament; GIKI, Pakistan). For dielectric measurements through impedance analyzer (microstate), both sides of each pellet were coated with silver to form parallel-plate capacitors. The relative permittivity ε_r was calculated from ε_r =

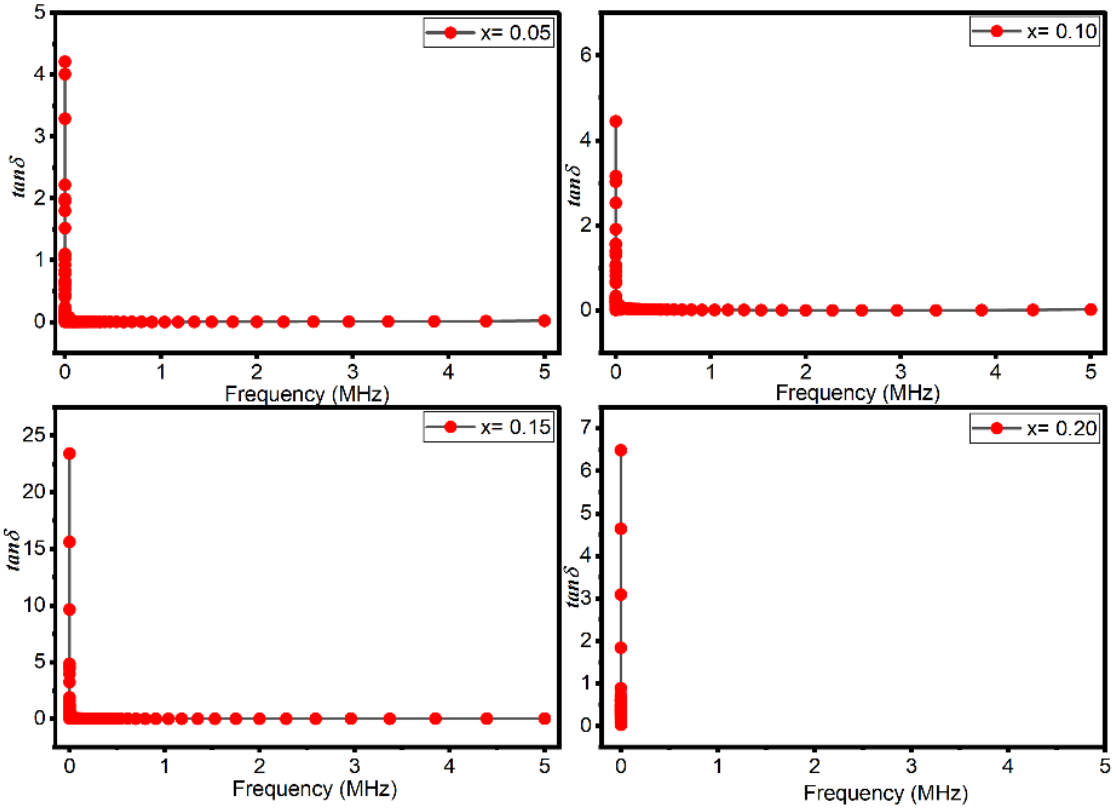

Figure 5. Tan δ function of ceramic sample $(1\text{-}x)$STO–xCZO ($x = 0.05, 0.10, 0.15, 0.20$).

$Ct/(\varepsilon_0 A)$, where C is the measured capacitance, t is the sample thickness, A is the electrode area, and $\varepsilon_0 = 8.854\,19 \times 10^{-12}\,\mathrm{F/m}$.

3 Results and Discussion

X-ray diffraction patterns of $(1\text{-}x)$STO–xCZO ceramics ($x = 0.05$, 0.10, 0.15, 0.20) measured at room temperature are shown in Figure 1. All compositions exhibit sharp reflections, indicating good crystallinity. Within the detection limit of the available XRD setup, no secondary phases are reported, supporting the formation of a single-phase solid solution across the studied composition range. The patterns are indexed to a cubic perovskite structure, consistent with the reference pattern used, and the lattice constant is reported as $a = b = c \approx 3.92$ Å for the cubic phase.

Room-temperature Raman spectra recorded in the range 0–1200 cm^{-1} are presented in Figure 2. Multiple bands are observed and discussed in the source document in terms of three spectral regions, including low-wavenumber features associated with A-site-related vibrations and modes linked with B–O bonding and BO_6 octahedral units. In the assignments given, the low-frequency band in the 0–190 cm^{-1} region is attributed to Zr–O vibrations, while bands in the 200–300 cm^{-1} region are attributed to Zr–O bending. The bands in the A-site regions A1 and B-mode are assigned to A–O vibrations, which are influenced by the mismatch in the valence of the cations. The presence of these Raman features is used in the manuscript to support local structural effects associated with CZO incorporation into the STO lattice.

SEM micrographs of polished and thermally etched ceramics are shown in Figure 3. For $x = 0.05, 0.10$, and 0.15, the microstructure is described as porous, with a reported average grain size of $0.51, 0.50, 0.48\,\mu$m, respectively. With increasing CZO content, the grain size is reported to decrease slightly, and the microstructure becomes more compact; the $x = 0.20$ composition is described as comparatively denser with average grain size of about $0.47\,\mu$m, with reduced visible porosity relative to lower-x samples. This densification trend is consistent with the improved dielectric-loss behavior noted for the highest CZO content.

The frequency dependence of relative permittivity ε_r for all compositions is shown in Figure 4. For each sample, ε_r decreases with increasing frequency, consistent with dielectric relaxation behavior and the reduced ability of polarization mechanisms to follow the alternating field at higher frequencies. Increasing the concentration of CZO decreases ε_r overall and

modifies the loss response: loss tangent ($\tan\delta$) is reported to be higher at low frequencies and then to decrease with increasing frequency as shown in Figure 5. Compared with the lower-x samples, $x = 0.20$ shows a clearer reduction in low-frequency loss. This reduced low-frequency $\tan\delta$ for $x = 0.20$ is interpreted in this article as indicating improved electrical resistivity and is discussed together with the more compact microstructure observed for this composition.

4 Conclusion

Lead-free (1-x)STO-xCZO ceramics with $x = 0.05, 0.10, 0.15,$ and 0.20 were fabricated using a conventional solid-state route with calcination at 1000 °C and high-temperature sintering (reported up to 1400 °C). X-ray diffraction confirms formation of a single-phase cubic perovskite structure for all compositions within the detection limit of the instrument, indicating incorporation of CZO into the STO lattice over the studied range. Raman spectra show composition-dependent vibrational features consistent with the perovskite lattice and Zr-O-related modes, supporting local structural changes associated with CZO addition. SEM analysis shows porous microstructures at lower CZO contents ($x = 0.05$–0.15), while increasing CZO content slightly reduces grain size and produces a more compact microstructure, most evident for $x = 0.20$. Dielectric measurements show clear frequency dispersion for all samples, with ε_r decreasing as frequency increases. Overall, CZO addition slightly decreases ε_r with the decreasing dielectric-loss behavior at higher x; in particular, $x = 0.20$ shows reduced low-frequency tanδ, consistent with enhanced resistivity and improved densification (95% of the theoretical density). These results show that composition control in the STO-CZO system can be used to tune microstructure and dielectric response in lead-free perovskite ceramics for dielectric and energy-storage-relevant applications.

Data Availability Statement

Data will be made available on request.

Funding

This work was supported without any funding.

Conflicts of Interest

The authors declare no conflicts of interest.

AI Use Statement

The authors declare that no generative AI was used in the preparation of this manuscript.

Ethical Approval and Consent to Participate

Not applicable.

References

[1] Khan, A., Ali, A., & Khan, I. (2021). Sintering behavior and microwave dielectric properties of CaTi1-x (Nb1/2Al1/2)xO3. *Synthesis and Sintering, 1*(3), 197-201. [CrossRef]

[2] Yang, H., Yan, F., Lin, Y., & Wang, T. (2017). Improvement of dielectric and energy storage properties in SrTiO3-based lead-free ceramics. *Journal of Alloys and Compounds, 728*, 780-787. [CrossRef]

[3] Petrov, P. K., Carlsson, E. F., Larsson, P., Friesel, M., & Ivanov, Z. G. (1998). Improved SrTiO3 multilayers for microwave application: Growth and properties. *Journal of Applied Physics, 84*(6), 3134-3140. [CrossRef]

[4] Shende, R. V., Krueger, D. S., Rossetti, G. A., & Lombardo, S. J. (2001). Strontium zirconate and strontium titanate ceramics for high-voltage applications: synthesis, processing, and dielectric properties. *Journal of the American Ceramic Society, 84*(7), 1648-1650. [CrossRef]

[5] Parida, S., Rout, S. K., Subramanian, V., Barhai, P. K., Gupta, N., & Gupta, V. R. (2012). Structural, microwave dielectric properties and dielectric resonator antenna studies of Sr (ZrxTi1-x) O3 ceramics. *Journal of Alloys and Compounds, 528*, 126-134. [CrossRef]

[6] Yu, Z., Ang, C., & Cross, L. (1999). Oxygen-vacancy-related dielectric anomalies in La: SrTiO3. *Applied Physics Letters, 74*(20), 3044-3046. [CrossRef]

[7] Ang, C., Yu, Z., & Cross, L. (2000). Oxygen-vacancy-related low-frequency dielectric relaxation and electrical conduction in Bi:SrTiO3. *Physical Review B, 62*(1), 228. [CrossRef]

[8] Wang, Z., Cao, M., Yao, Z., Song, Z., Li, G., Hu, W., ... & Liu, H. (2014). Dielectric relaxation behavior and energy storage properties in SrTiO3 ceramics with trace amounts of ZrO2 additives. *Ceramics International, 40*(9), 14127-14132. [CrossRef]

[9] Lu, Z., Zhang, H., Lei, W., Sinclair, D. C., & Reaney, I. M. (2016). High-figure-of-merit thermoelectric La-doped A-site-deficient SrTiO3 ceramics. *Chemistry of Materials, 28*(3), 925-935. [CrossRef]

[10] Alay-e-Abbas, S. M., Nazir, S., Cottenier, S., & Shaukat, A. (2017). Evaluation of thermodynamics, formation energetics and electronic properties of vacancy defects in CaZrO3. *Scientific Reports, 7*(1), 8439. [CrossRef]

[11] Levin, I., Amos, T. G., Bell, S. M., Farber, L., Vanderah, T. A., Roth, R. S., & Toby, B. H. (2003). Phase equilibria, crystal structures, and dielectric anomaly in the BaZrO3–CaZrO3 system. *Journal of Solid State Chemistry, 175*(2), 170-181. [CrossRef]

[12] Hou, Z. (2008). Ab initio calculations of elastic modulus and electronic structures of cubic CaZrO3. *Physica B: Condensed Matter, 403*(17), 2624-2628. [CrossRef]

[13] Pollet, M., Marinel, S., & Desgardin, G. (2004). CaZrO3, a Ni-co-sinterable dielectric material for base metal-multilayer ceramic capacitor applications. *Journal of the European Ceramic Society, 24*(1), 119-127. [CrossRef]

[14] Prasanth, C., Kumar, H. P., Pazhani, R., Solomon, S., & Thomas, J. (2008). Synthesis, characterization and microwave dielectric properties of nanocrystalline CaZrO3 ceramics. *Journal of Alloys and Compounds, 464*(1-2), 306-309. [CrossRef]

[15] Wang, X., Hu, Q., Wang, Z., Zhou, F., & Li, L. (2022). High temperature dielectric relaxation and energy storage properties achieved in the CaZrO3–SrTiO3 composite ceramics. *Modern Physics Letters B, 36*(31), 2250160. [CrossRef]

Akbar Khan received the Ph.D. degree in Physics from Abdul Wali Khan University, Mardan, Pakistan, with a specialization in electromagnetic interference (EMI) shielding materials. He also completed his M.Phil. and Bachelor's degrees in Physics from the same institution. His doctoral research focused on the design, development, and characterization of advanced materials for effective EMI shielding, addressing key challenges in modern electronic and communication systems. He has extensive hands-on experience in experimental techniques, data analysis, and scientific writing. His research interests include electromagnetic compatibility and advanced functional materials. He is committed to contributing to scientific innovation and applying his expertise to address real-world technological challenges. He aspires to pursue a career in research, academia, or industry, with a focus on developing cutting-edge solutions in physics and materials science. (Email: akbar.khan@awkum.edu.pk)

Basit Ahmad completed his Master's degree in Physics with a specialization in Materials Science from Abdul Wali Khan University, Mardan, Pakistan. He received his Bachelor's degree in Physics from Government Degree College Wari, affiliated with Shaheed Benazir Bhutto University, Sheringal, Dir Upper. His academic training has provided him with a strong foundation in both theoretical and applied aspects of physics, with particular emphasis on the study and development of advanced materials. (Email: basitmayar444@gmail.com)